Multi-body NRSfM (NRSfM Challenge 2017)

Suryansh Kumar, Yuchao Dai, Hongdong Li

July 26, 2017

Content

Introduction

Why Multi-body NRSfM Representation?

- Real-world scene consist of multiple deforming objects. For example: pedestrians, soccer match, human interaction and etc.

Goal:

- To segment and reconstruct multiple deforming objects in a scene, simultaneously.

Baseline strategy:

- Two-stage approach:
  - motion segmentation followed by non-rigid reconstruction
  - non-rigid reconstruction followed by motion segmentation.

Why unified approach?

- To better exploit the inherent structure of the problem
  - ⇒ Motion segmentation benefits reconstruction
  - ⇒ Reconstruction benefits motion segmentation
- Both tasks can be solved efficiently within a single optimization.
- Computationally and numerically efficient.

Spatial-Temporal Representation

To exploit the intrinsic structure both spatially and temporally, we propose the spatial-temporal representation for complex non-rigid reconstruction.

- Spatial Clustering $\Rightarrow$ Provides motion segmentation cues
- Temporal Clustering $\Rightarrow$ Benefits 3D reconstruction

• Spatial Clustering exploits Trajectory space.
• Temporal Clustering exploits Shape space.

Trajectory Space

Classical NRSfM Representation

$$\mathbf{W} = \mathbf{RS}, \text{ where } \mathbf{R} \in \mathbb{R}^{2F \times 3F}, \mathbf{S} \in \mathbb{R}^{3F \times P} \tag{1}$$

$\mathbf{W} \in \mathbb{R}^{2F \times P} \Rightarrow$ Measurement matrix.
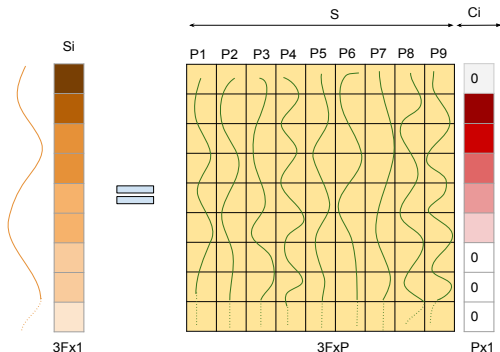$\mathbf{S} \Rightarrow$ Shape matrix.
$\mathbf{R} \Rightarrow$ Rotation matrix (Orthographic Camera Model).

Trajectory Space

Representation of multiple non-rigid deformation in the trajectory space.

$$S = SC_1, diag(C_1) = 0, 1^T C_1 = 1^T.$$
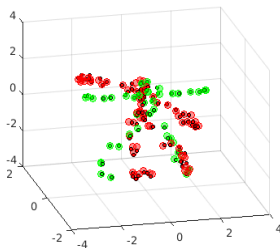$$S \in \mathbb{R}^{3F \times P}, C_1 \in \mathbb{R}^{P \times P}. \tag{2}$$

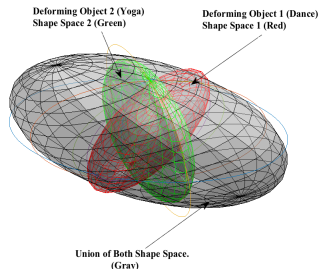**Figure:** Illustration of trajectory space

Shape Space

Representation of multiple non-rigid deformation in the shape space.

$$S^\sharp = S^\sharp C_2, diag(C_2) = 0, 1^T C_2 = 1^T.$$
$$S^\sharp \in \mathbb{R}^{3P \times F}, C_2 \in \mathbb{R}^{F \times F}. \qquad (3)$$

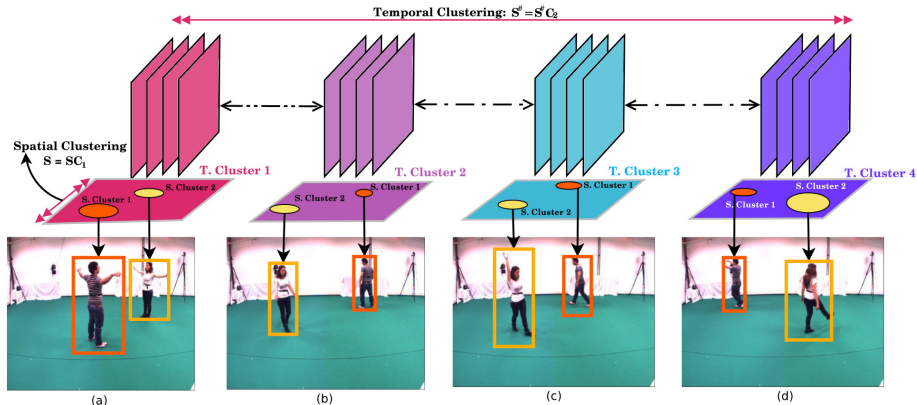$\Rightarrow$ Intuition [Cluster distinct activity (Ex: Dance, Yoga)]

(a)   (b)

Figure: Intuition of spatial-temporal clustering.

Joint Optimization Formulation

- Objective from the trajectory space

$$\underset{C_1}{\text{minimize }} \lambda_1 \|C_1\|_1 + \frac{(1 - \lambda_1)}{2} \|C_1\|_F^2$$

subject to:

$$S = SC_1, \operatorname{diag}(C_1) = 0, 1^T C_1 = 1^T, \lambda_1 \in [0, 1].$$

(4)

- Objective from the shape space

$$\underset{C_2}{\text{minimize }} \lambda_3 \|C_2\|_1 + \frac{(1 - \lambda_3)}{2} \|C_2\|_F^2$$

subject to:

$$S^\sharp = S^\sharp C_2, \operatorname{diag}(C_2) = 0, 1^T C_2 = 1^T, \lambda_3 \in [0, 1].$$
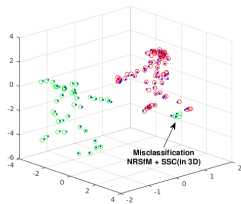
(5)

Joint Optimization Formulation

- Overall Objective $\Rightarrow$ solved using ADMM

$$\underset{S, C_1, C_2}{\text{minimize}} \ \frac{1}{2}\|W - RS\|_F^2 + \lambda_1\|C_1\|_1 + \frac{1 - \lambda_1}{2}\|C_1\|_F^2 + \lambda_2\|S^\sharp\|_* +$$

$$\lambda_3\|C_2\|_1 + \frac{1 - \lambda_3}{2}\|C_2\|_F^2.$$

subject to:

$$S = SC_1, S^\sharp = S^\sharp C_2,$$

$$1^T C_1 = 1^T, 1^T C_2 = 1^T,$$

$$\mathrm{diag}(C_1) = 0, \mathrm{diag}(C_2) = 0,$$

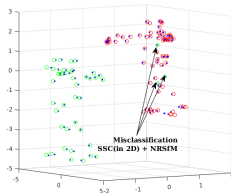$$\lambda_1, \lambda_3 \in [0, 1].$$

(6)

where $S^\sharp \in \mathbb{R}^{3P \times F}$, $C_1 \in \mathbb{R}^{P \times P}$, and $C_2 \in \mathbb{R}^{F \times F}$ and $\lambda_1, \lambda_2, \lambda_3$ are the trade-off parameters.

Experiments and Results

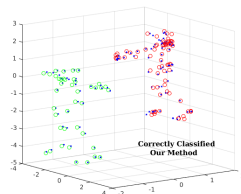- Advantage over two stage approach

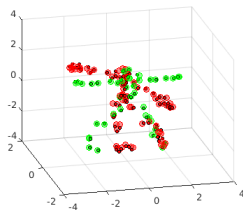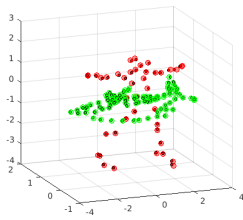(a) NRSfM ⇒ SSC [2]   (b) SSC [2] ⇒ NRSfM   (c) Our approach

Qualitative results on synthetic sequence
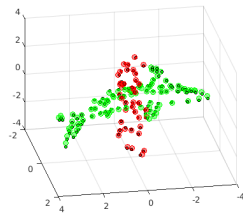
- Two deforming objects are intersecting each other.

(d) Dance-Yoga   (e) Shark-Stretch   (f) Shark-Yoga

Qualitative results(Cont.)

- Two deforming objects are well separated in space.
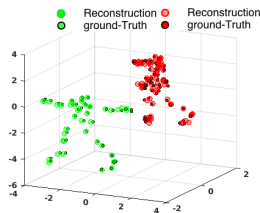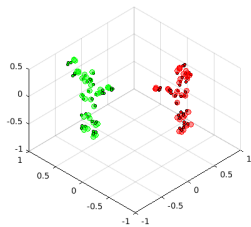
(g) Dance-Yoga   (h) UMPM p3_ball_1   (i) UMPM p4_meet_12
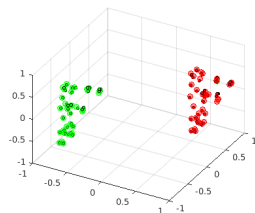
UMPM dataset [10] is composed of real-image tracks.

Quantitative Results on benchmark real-dataset

Datasets	BMM[1]	PND[9]	Zhu et al.[11]	Kumar et al.[8]	Ours
p2_free_2	0.1973	0.1544	**0.1142**	0.1992	0.1171
p2_grab_2	0.2018	0.1570	0.0960	0.2080	**0.0822**
p3_ball_1	0.1356	0.1477	0.0832	0.1348	**0.0810**
p4_meet_12	0.0802	0.0862	0.0972	0.0821	**0.0815**
p4_table_12	0.2313	0.1588	0.1322	0.2313	**0.0994**

Table: Performance comparison on real benchmark UMPM dataset [10] (showing relative 3D reconstruction error).

Quantitative Results on benchmark real-dataset

Datasets	BMM[1]	PND[9]	Zhu et al.[11]	Kumar et al.[8]	Ours
Face Seq.1	0.078	0.077	0.082	0.075	**0.073**
Face Seq.2	0.059	0.062	0.063	**0.050**	0.052
Face Seq.3	0.042	0.051	0.057	**0.038**	0.039
Face Seq.4	0.049	0.041	0.056	0.044	**0.040**

Table: Performance comparison on real benchmark dense face dataset [3] (showing relative 3D reconstruction error).

Evaluation result on NRSfM challenge dataset for test frame.

- Mean RMS (in mm) for orthogonal category.

Datasets	Articulated	Balloon	Paper	Stretch	Tearing
Our Method	10.15	10.64	15.78	9.96	14.17

Table: Performance on the NRSFM challenge dataset on all provided sequence for *single* test image provided by the challenge organizers.

- Note: We submitted results for two methods. Numerically, both of them performed with similar reconstruction accuracy [8] [7].

Performance comparison with other top 3 performing algorithms on NRSfM challenge dataset.

- Mean RMS (in mm) for orthogonal category.

Datasets	Articulated	Balloon	Paper	Stretch	Tearing	Mean
Multibody[7]	45.51	**14.55**	**22.88**	**18.30**	21.98	**24.64**
CSF2 [5]	**35.51**	19.01	33.95	23.22	18.77	26.09
RIKS [6]	42.11	18.45	32.18	22.88	18.12	26.75
KSTA [4]	36.63	24.88	31.96	24.25	**17.59**	26.86

Table: Note: These evaluations were done by the organizers of NRSfM challenge at CVPR 2017.

Award

Thanks

References I

[1] Y. Dai, H. Li, and M. He.
A simple prior-free method for non-rigid structure-from-motion factorization.
International Journal of Computer Vision, 107(2):101–122, 2014.

[2] E. Elhamifar and R. Vidal.
Sparse subspace clustering: Algorithm, theory, and applications.
IEEE Transactions on Pattern Analysis and Machine Intelligence, 35(11):2765–2781, 2013.

[3] R. Garg, A. Roussos, and L. Agapito.
Dense variational reconstruction of non-rigid surfaces from monocular video.
In *Proc. IEEE Conf. Computer Vision and Pattern Recognition*, pages 1272–1279, 2013.

[4] P. Gotardo and A. Martinez.
Kernel non-rigid structure from motion.
In *Proc. IEEE Int'l Conf. Computer Vision*, pages 802–809, 2011.

[5] P. Gotardo and A. Martinez.
Non-rigid structure from motion with complementary rank-3 spaces.
In *Proc. IEEE Conf. Computer Vision and Pattern Recognition*, pages 3065–3072, 2011.

[6] O. C. Hamsici, P. F. Gotardo, and A. M. Martinez.
Learning spatially-smooth mappings in non-rigid structure from motion.
In *European Conference on Computer Vision*, pages 260–273. Springer, 2012.

References II

[7] S. Kumar, Y. Dai, and H.Li.
     Spatio-temporal union of subspaces for multi-body non-rigid structure-from-motion.
     Pattern Recognition, 71:428–443, May 2017.

[8] S. Kumar, Y. Dai, and H. Li.
     Multi-body non-rigid structure-from-motion.
     In *3D Vision (3DV), 2016 Fourth International Conference on*, pages 148–156. IEEE, 2016.

[9] M. Lee, J. Cho, C.-H. Choi, and S. Oh.
     Procrustean normal distribution for non-rigid structure from motion.
     In *Proc. IEEE Conf. Computer Vision and Pattern Recognition*, pages 1280–1287, 2013.

[10] N. van der Aa, X. Luo, G. Giezeman, R. Tan, and R. Veltkamp.
     Umpm benchmark: A multi-person dataset with synchronized video and motion capture data for evaluation of articulated human motion and interaction.
     In *Computer Vision Workshops (ICCV Workshops), 2011 IEEE International Conference on*, pages 1264–1269, Nov 2011.

[11] Y. Zhu, D. Huang, F. De La Torre, and S. Lucey.
     Complex non-rigid motion 3d reconstruction by union of subspaces.
     In *IEEE Conference on Computer Vision and Pattern Recognition*, pages 1542–1549, 2014.